Please cite this article in press as: Cheng et al., Influence of very-long-chain polyunsaturated fatty acids on membrane structure and dynamics, Biophysical Journal (2022), https://doi.org/10.1016/j.bpj.2022.06.015

Biophysical *Journal*
Article

Biophysical Society

Influence of very-long-chain polyunsaturated fatty acids on membrane structure and dynamics

Victoria Cheng,[1] Rameshu Rallabandi,[1] Aruna Gorusupudi,[2] Steven Lucas,[1] Gregory Rognon,[2] Paul S. Bernstein,[2] Jon D. Rainier,[1] and John C. Conboy[1,*]

[1]Department of Chemistry, University of Utah, Salt Lake City, Utah and [2]Department of Ophthalmology and Visual Sciences, John A. Moran Eye Center, University of Utah, Salt Lake City, Utah

ABSTRACT The unique attributes of very-long-chain polyunsaturated fatty acids (VLC-PUFAs), their long carbon chains ($n > 24$) and high degree of unsaturation, impart unique chemical and physical properties to this class of fatty acids. The changes imparted by VLC-PUFA 32:6 n-3 on lipid packing and the compression moduli of model membranes were evaluated from π-A isotherms of VLC-PUFA in 1,2-distearoyl-sn-3-glycero-phosphocholine (DSPC) lipid monolayers. To compare the attractive or repulsive forces between VLC-PUFA and DSPC lipid monolayers, the measured mean molecular areas (MMAs) were compared with the calculated MMAs of an ideal mixture of VLC-PUFA and DSPC. The presence of 0.1, 1, and 10 mol % VLC-PUFA shifted the π-A isotherm to higher MMAs of the lipids comprising the membrane and the observed positive deviations from ideal behavior of the mixed VLC-PUFA:DSPC monolayers correspond to repulsive forces between VLC-PUFAs and DSPC. The MMA of the VLC-PUFA component was estimated using the measured MMAs of DSPC of 47.1 $\pm$ 0.7 Å^2/molecule, to be 15,000, 1100, and 91 Å^2/molecule at 0.1, 1, and 10 mol % VLC-PUFA:DSPC mixtures, respectively. The large MMAs of VLC-PUFA suggest that the docosahexaenoic acid tail reinserts into the membrane and adopts a nonlinear structure in the membrane, which is most pronounced at 0.1 mol % VLC-PUFA. The presence of 0.1 mol % VLC-PUFA:DSPC also significantly increased the compression modulus of the membrane by 28 mN/m compared with a pure DSPC membrane. The influence of VLC-PUFA on lipid "flip-flop" was investigated by sum-frequency vibrational spectroscopy. The incorporation of 0.1 mol % VLC-PUFA increased the DSPC flip-flop rate fourfold. The fact that VLC-PUFA promotes lipid translocation is noteworthy as retinal membranes require a high influx of retinoids which may be facilitated by lipid flip-flop.

SIGNIFICANCE The importance of VLC-PUFAs to retinal health is an important discovery, but the underlying biophysical mode of action is not well understood. The unique attributes of VLC-PUFAs, their long carbon chains ($n > 24$) and high degree of unsaturation, impart unique chemical and physical properties to this class of fatty acids. The goal of studies presented in this manuscript aim to systematically explore the biophysical effects of VLC-PUFAs on the packing, morphology, and mechanical properties of lipid membranes as a means of deciphering their biophysical mechanism of action in restoring biological function to retinal cell membranes.

INTRODUCTION

Retinal membranes are comprised of a variety of unique phospholipids, proteins, and fatty acids. The presence of one particular group of fatty acids, known as very-long-chain polyunsaturated fatty acids (VLC-PUFAs), was first identified over three decades ago, and they have been implicated in maintaining healthy retinal function, particularly rod photoreceptors (1–5). Structurally, VLC-PUFAs are unique in that they contain a saturated acyl fragment containing between 12 and 20 carbons and a methylene-interrupted polyunsaturated fragment (1,6,7). The unsaturated terminal region of VLC-PUFAs found in the retina are predominantly n-3 and n-6 with four to six conjugated double bonds in the fatty acid chain. The retinal rod outer segment (ROS) membrane is enriched in VLC-PUFAs with the composition of 22:6 n-3, 32:6 n-3, and 34:6 n-3 (6,8,9). These VLC-PUFAs make up less than 2% of the total fatty acid content of the membrane either as either free fatty acids or as components of the lipids comprising the ROS (1,10). The structure of one of the more common VLC-PUFAs (C32:6 n-3) found in retinal tissue is shown in Fig. 1.

Submitted January 11, 2022, and accepted for publication June 10, 2022.

*Correspondence: conboy@chem.utah.edu

Editor: Sarah L. Veatch.

https://doi.org/10.1016/j.bpj.2022.06.015

Please cite this article in press as: Cheng et al., Influence of very-long-chain polyunsaturated fatty acids on membrane structure and dynamics, Biophysical Journal (2022), https://doi.org/10.1016/j.bpj.2022.06.015

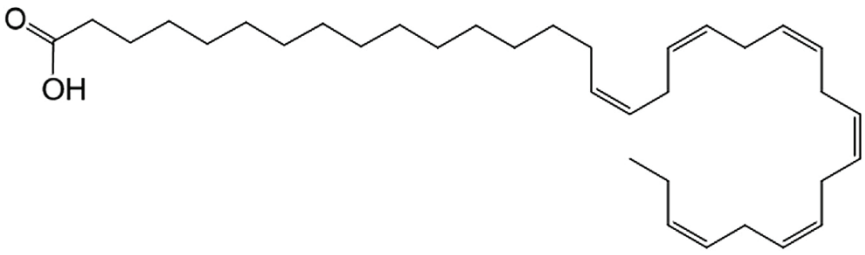

FIGURE 1 Structure of the VLC-PUFA (C32:6 n-3) used in this study.

VLC-PUFAs are produced in retinal cells through the action of the fatty acid elongase enzyme ELOVL4 which extends the precursor long-chain polyunsaturated fatty acid (LC-PUFA) chains (11). In the retina, deficiencies in VLC-PUFAs stem generally from either low dietary intake of precursor LC-PUFAs or altered activity of ELOVL4 which synthesizes VLC-PUFAs in the endoplasmic reticulum (12,13). VLC-PUFAs are crucial for proper functioning of the retina, with reduction in VLC-PUFAs, due to genetic mutations in ELOVL4, resulting in a macular dystrophy known as Stargardt-3 disease (14,15). In particular, Bernstein's group has measured a significantly higher distribution of VLC-PUFAs in mouse retinas versus other tissues and cell types and has also demonstrated their potential role in reversing macular degeneration and dystrophies in the retina (4,14,16,17). Furthermore, conditional knockouts of the ELOVL4 gene in mice showed that deficiencies in VLC-PUFAs resulted in disorganization of the outer plexiform layer, mislocalization of glutamatergic vesicles to the outer nuclear layer, and reduced longevity of rods in mouse retinas (18). At the cellular membrane level, there is growing consensus that VLC-PUFAs are pivotal in stabilizing rhodopsin in the rod photoreceptor cells. Aveldano and co-workers has found that phosphocholines containing VLC-PUFA interact strongly with rhodopsin, supported by a VLC-PUFA-rhodopsin complex after extraction by hexanes from lyophilized disks (19–23). They proposed that the structural flexibility afforded by the polyunsaturated distal tail of VLC-PUFAs provides support for the transmembrane helices of rhodopsin in the membrane. In addition, molecular dynamic simulations of 1-stearoyl-2-docosahexaenoyl-*sn*-glycero-3-phosphocholine interactions with rhodopsin demonstrated that the transmembrane helices of rhodopsin preferentially associated with the docosahexaenoic acid (DHA) (22:6 n-3) tail (21). In addition, the hybrid saturated/unsaturated structure and the elongated chain length of VLC-PUFAs are also believed to impart increased membrane fluidity and help stabilize the curved membrane structure of the photoreceptor outer segments in retinal cells (18,19,24).

In a recent publication, we demonstrated that supplementation with a synthetic VLC-PUFA (32:6 n-3) in wild-type and ELOVL4 conditional knockout mice led to increased concentration of VLC-PUFA in the retina and improved retinal function (25). These studies were made possible by a novel synthetic route to the VLC-PUFAs such that they could be prepared in sufficient quantities for in vitro and in vivo studies (25). The availability of sufficient quantities of synthetically pure VLC-PUFA also provides the means to assess the biophysical properties of VLC-PUFAs on phospholipid membranes in a controlled and systematic manner.

The studies herein were motivated by the need to characterize a biologically rare but influential membrane component found in the membrane of retinal cells, VLC-PUFAs, in an attempt to investigate their impact on lipid membrane properties. In particular, the changes imparted by VLC-PUFAs on lipid packing and the compression moduli of model membranes were evaluated from pressure-area (π-A) isotherms of VLC-PUFA (32:6 n-3) at 0.1, 1, and 10 mol % in lipid monolayers containing 1,2-distearoyl-*sn*-3-glycero-phosphocholine (DSPC). DSPC was chosen as the lipid matrix in these studies as the saturated acyl chains of DSPC are commensurate with the proximal saturated fatty portion of VLC-PUFA. In addition, deuterated analogs of DSPC, which are required for the detailed spectroscopic and dynamics studies, were commercially available in high purity. From the π-A isotherms the changes in DSPC packing and compression moduli of the membranes were examined. Specifically, the compression moduli of VLC-PUFA:DSPC mixtures were determined, as it has been postulated that VLC-PUFAs may modulate membrane rigidity (26,27).

In addition to the static perturbations to a lipid membrane, the effect on lipid translocation (flip-flop) was also investigated by sum-frequency vibrational spectroscopy (SFVS). Lipid translocation in retinal membranes is required for proper photoreceptor response to the massive influx of retinoids after photopigment bleaching and the proper organization and dynamics of rhodopsin. VLC-PUFA mediated lipid flip-flop may provide an alternative nonenzymatic mechanism for retinoid translocation in photoreceptors which does not require the ABCA4 enzyme (28), which could facilitate proper retinal functioning.

MATERIALS AND METHODS

Materials

All materials were used as received, unless otherwise noted. DSPC, and 1,2-distearoyl-d_{70}-sn-3-glycero-phosphocholine ($DSPCd_{70}$) were purchased from Avanti Polar Lipids (Alabaster, AL) and used without further purification. NaCl, NaOH, and HCl were purchased from Macron Chemicals (Center Valley, PA). Sodium phosphate anhydrous (dibasic), sodium phosphate

Please cite this article in press as: Cheng et al., Influence of very-long-chain polyunsaturated fatty acids on membrane structure and dynamics, Biophysical Journal (2022), https://doi.org/10.1016/j.bpj.2022.06.015

(monobasic), and hydrogen peroxide were purchased from Fisher Scientific (Pittsburgh, PA). DHA, chloroform and deuterium oxide were purchased from Sigma-Aldrich Millipore (St. Louis, MO). PBS buffer consisting of 100 mM NaCl, 10 mM NaH_2PO_4, and 40 mM Na_2HPO_4 prepared in Nanopure water with a minimum resistivity of 18.2 MΩ·cm (Barnstead Thermolyne, Dubuque, IA) was used in all experiments. The pH was adjusted using either 2 M NaOH or 2 M HCl. UV-IR grade fused silica trapezoidal prisms used as the membrane support were purchased from Almaz Optics (Marlton, NJ) and cleaned thoroughly before use. Prisms were first placed in an UV-ozone cleaner (Jetlight, Irvine, CA) for 30 min, followed by submersion in a solution of 30% (v/v) H_2O_2 and 70% (v/v) H_2SO_4 for a minimum of 30 min. (*Caution*: *this is a highly corrosive solution that reacts violently with organic solvents. Take extreme caution and care when handling the solution*.) The prisms were rinsed thoroughly with Nanopure water before drying in an oven at 120°C for at least 15 min. Once the prisms were dry, they were cleaned once more with an argon plasma (Harrick Scientific, Ithaca, NY) for 2 min.

VLC-PUFA (C32:6 n-3) Synthesis

VLC-PUFA (C32:6 n-3) was synthesized via the method described by Wade et al. (29). In the discussion that follows the use of VLC-PUFA refers to the C32:6 n-3 form. VLC-PUFA was stored at −80°C under nitrogen before use to prevent oxidation.

Methods

π-A isotherms

π-A isotherms were collected using a Langmuir trough (KSV, Helsinki, Finland). PBS was used as the subphase for all isotherms. Stock solutions of pure VLC-PUFA, pure DHA, pure DSPC, and DSPC containing 0.1, 1, or 10 mol % VLC-PUFA or DHA were spread at the air/water interface and allowed to equilibrate for 15 min before compression to allow for solvent evaporation. The monolayers were compressed at a rate of 2 mm/min at 22 ± 1°C and repeated in triplicate. The averaged isotherms were smoothed using a 100-point rolling average.

As a control, π-A isotherms were also collected with an argon purged subphase. No measurable differences in the measured isotherms or calculated compression moduli were observed. Unless otherwise noted, the data were collected under ambient conditions.

Bilayer preparation

Planar supported lipid bilayers (PSLBs) used in this study were prepared using the Langmuir-Blodgett/Langmuir-Schaefer (LB/LS) method, the details of which are presented elsewhere (30). In brief, the cleaned SiO_2 prisms were submerged in PBS. Afterward, 0.1 mol % VLC-PUFA in $DSPCd_{70}$ was spread over the air/water interface and allowed to equilibrate for 15 min. Afterward, the monolayer was compressed to 30 mN/m at a rate of 4 mm/min, and the surface pressure was allowed to stabilize for another 5 min. The prism was then withdrawn at a rate of 3 mm/min to deposit the LB layer. The subphase was removed, and the trough was cleaned using methanol, isopropanol, and water. Following this, fresh PBS was introduced into the trough, and 0.1 mol % VLC-PUFA in DSPC was spread at the air/water interface. The monolayer was then compressed to 30 mN/m at a rate of 4 mm/min. The prism was rotated horizontally so that the LB layer was parallel to the air/water interface. The prism was submerged through the monolayer, depositing the LS layer resulting in the formation of a fully assembled bilayer. From this point forward, the bilayer was maintained in an aqueous environment. The prism was transferred to a custom Teflon flow-cell that was equipped with ports to allow for solution exchange and a K-type thermocouple to monitor the temperature.

DSPC flip-flop kinetics

SFVS, a complementary method for studying lipid flip-flop, has been shown to be a useful and direct method for probing lipid translocation in model membranes (31). Similar to SANS (32) and NR (33) methods for measuring lipid flip-flop, SFVS substitutes a fraction of lipids with deuterated lipids and does not require the use of bulky spin or fluorescent labels. The foundations of SFVS are described in detail elsewhere, and only a brief description follows (34). SFVS is a second-order nonlinear spectroscopy that is forbidden in media with inversion symmetry but allowed at interfaces where the inversion symmetry of the bulk is broken. To obtain a SFVS, a laser at a fixed visible wavelength is spatially and temporally overlapped with a tunable mid-IR beam at an interface, whereby a beam at the sum of the incident frequencies is generated:

$$\omega_{SF} = \omega_{vis} + \omega_{IR} \tag{1}$$

The SFVS intensity is given by

$$I_{SF} = \left|\tilde{f}_{SF} f_{vis} f_{ir} \chi^{(2)}\right|^2 \tag{2}$$

where $\tilde{f}_{SF}$, f_{vis}, and f_{ir} are the Fresnel coefficients of the electric field intensities of the sum-frequency, visible, and *IR* beams, respectively. $\chi^{(2)}$ is the second-order nonlinear susceptibility, which is the sum of the resonant ($\chi^{(2)}_R$) and nonresonant ($\chi^{(2)}_{NR}$) susceptibilities:

$$I_{SF} \propto \left|\left(\chi^{(2)}_{NR} + \sum_v \frac{A_v}{\omega_v - \omega_{IR} - i\Gamma}\right)\right|^2 \tag{3}$$

where A_v is the product of the *IR* and Raman transition probabilities and the strength of the transition of the υ vibrational mode, ω_v is the frequency of the vibrational mode, ω_{IR} is the frequency of the incident *IR* beam, and Γ is the intrinsic linewidth of the vibrational transition. In the specific case of lipid bilayers, we use the methyl symmetric stretch (CH_3 ν_s) intensity from the termini of the fatty acid chains of the lipids as an indicator of bilayer asymmetry. This is achieved by preparing phospholipid bilayers with perdeuterated and perhydrogenated lipids in each leaflet, respectively. The intensity of the CH_3 ν_s stretch can be described in terms of the effective nonlinear susceptibility ($\chi^{(2)}_{eff}$):

$$\chi^{(2)}_{eff} = \frac{N_{distal}}{\varepsilon_0}\langle\beta^{CH_3\nu_s}_{ijk}\rangle - \frac{N_{proximal}}{\varepsilon_0}\langle\beta^{CH_3\nu_s}_{ijk}\rangle + \chi^{(2)}_{NR} \tag{4}$$

where N_{distal} and $N_{proximal}$ are the proportion of proteated lipids in the leaflets, proximal or distal, to the solid support, and β_{ijk} is the molecular hyperpolarizability. The measured sum-frequency intensity is related to the measured intensity of the CH_3 ν_s through the following expression:

$$I_{SF} \propto \left(N_{distal} - N_{proximal}\right)^2 \tag{5}$$

Initially, the fraction of proteated lipids in each leaflet are $N_{distal} = 1$ and $N_{proximal} = 0$ in the as-prepared bilayer, and interleaflet lipid exchange is described by the equilibrium:

$$N_{distal} \underset{k_-}{\overset{k_+}{\rightleftharpoons}} N_{proximal} \tag{6}$$

where k_+ and k_- denote the forward and backward rates of flip-flop. As lipids exchange between leaflets over time, the change in N_{distal} with respect to time is expressed as:

$$\frac{dN_{distal}}{dt} = k_+ N_{distal} - k_- N_{proximal} \tag{7}$$

Please cite this article in press as: Cheng et al., Influence of very-long-chain polyunsaturated fatty acids on membrane structure and dynamics, Biophysical Journal (2022), https://doi.org/10.1016/j.bpj.2022.06.015

It has been previously shown that the rate of lipid flip-flop did not depend on the order of deposition (i.e., whether the proteated component is in the distal or proximal leaflet) (35). Thus, Eq. 5 becomes:

$$\frac{dN_{distal}}{dt} = -k(2N_{distal} - 1) \tag{8}$$

and the integrated rate expression is:

$$2N_{distal}(t) - 1 = e^{-2kt} \tag{9}$$

where $2N_{distal} - 1$ is the population difference of proteated components in each leaflet. From Eq. 4, the population difference between leaflets is related to the effective nonlinear susceptibility, so the time-dependent version of Eq. 4 is described as:

$$\chi^{(2)}_{eff} = |\chi_R|e^{i\varphi_1}e^{-2kt} + |\chi_{NR}|e^{i\varphi_2} \tag{10}$$

where $|\chi_R|$ and $|\chi_{NR}|$ are the magnitudes of the complex resonant and nonresonant susceptibilities with phase angles of φ_1 and φ_2, respectively. When the resonant and nonresonant contributions are in or out of phase, the difference in the phase angles ($\Delta\varphi$) is taken as 0 or π, respectively. By substituting Eq. 10 into Eq. 2, the intensity of the CH_3 ν_s can be expressed as:

$$I_{CH_3\ \nu_s}(t) = I_{R,max}e^{-4kt} + 2\sqrt{I_r}\sqrt{I_{NR}}e^{-2kt}\cos(\Delta\varphi) + I_{NR} + I_{R,min} \tag{11}$$

where $I_{R,max}$ and $I_{R,min}$ are the maximum and minimum intensities of the CH_3 ν_s stretch, respectively. I_{NR} is the nonresonant background intensity, and for the model lipid bilayers on SiO_2, I_{NR} is extremely small at frequencies where CH vibrational modes are absent. Thus, I_{NR} can be removed from Eq. 11, which simplifies to:

$$I_{CH_3}(t) = I_{min} + I_{max}e^{-4kt} \tag{12}$$

where I_{max} is the initial signal from the as-prepared asymmetric bilayer and I_{min} accounts for the signal offset of the detection system.

After bilayer assembly, the flow-cell was flushed with PBS in D_2O to eliminate any spectral interference from the O-H bands from water. The spectrometer setup used in these studies is described in detail elsewhere (31). An initial spectrum was taken before kinetics measurements to ascertain bilayer formation. The spectrometer was then tuned to 2875 cm^{-1}, and the temperature of the flow cell was raised for the kinetics measurements. The flip-flop rate was obtained from the decay profiles by fitting Eq. 12 to the data.

RESULTS AND DISCUSSION

π-A isotherms

The impact of VLC-PUFA on DSPC membrane packing was evaluated from the π-A isotherms (Fig. 2). DSPC was chosen as the model lipid in these studies as it is well suited for exploring the VLC-PUFA perturbations via π-A isotherms and the availability of its dueterated analogs provides a means to assess the structural and kinetic perturbations induced by VLC-PUFA using SFVS. The studies presented herein could not be conducted on unsaturated lipid species as the required dueterated lipids are not commercially available. Although DSPC is not the most biologically rigorous model system, it does provide a means to assess VLC-PUFA lipid interactions in a systematic manner. For consistency, all mean molecular areas (MMAs) are compared at 20 mN/m. The collapse pressures of the pure DSPC and pure VLC-PUFA monolayers were determined to be 61 and 23 mN/m, respectively. The measured collapse pressure of DSPC is in agreement with a previously determined pressure of 60 mN/m (36). The collapse pressures of the 0.1, 1, and 10 mol % VLC-PUFA mixtures were determined to be 59, 62, 64 mN/m, respectively.

The π-A isotherms of DSPC:VLC-PUFA display a continuous smooth progression from low to high pressure as a function of MMA with an absence of discrete transitions or plateaus which are indicative of phase transitions or lipid segregation in the membrane. The most striking trend observed in the π-A isotherms is the large increase in the MMA upon the addition of 0.1 and 1 mol % VLC-PUFA in the DSPC membrane with an increase of 15 and 11 $Å^2$/lipid respectively over the MMA of DSPC (47 $Å^2$/lipid) alone, Fig. 3. At 10 mol % VLC-PUFA the change in the lipid packing is reduced to an increase of 4 $Å^2$/lipid. This is surprising given the much smaller MMA of pure VLC-PUFA at 20 mN/m of 36 $Å^2$/lipid.

To investigate the role of the polyunsaturated portion of VLC-PUFA (C32:6-n6) on the behavior observed in the π-A isotherms of VLC-PUFA + DSPC; isotherms of the structural analog of the pendent polyunsaturated chain, DHA (C22:6-n3), in DSPC were also measured, Fig. 2. The collapse pressure of a pure DHA monolayer was measured to be ~25 mN/m which is consistent with reported literature values (37). In addition to the collapse pressure, the π-A isotherms of DSPC:DHA closely resemble those of VLC-PUFA at pressures above 15 mN/m. However, at pressures below 15 mN/m, the binary 0.1 and 10 mol % DHA:DSPC mixtures show clear phase transitions with regions of phase segregation as noted by the plateau regions. Interestingly, 1 mol % DHA:DPSC does not exhibit this behavior. These observations suggest that the packing behavior of VLC-PUFA is shaped partially by the DHA-like pendent tail of VLC-PUFA, but the proximal saturated 14- carbon portion appears to eliminate the phase transitions and phase coexistence regions observed for DHA alone. However, the magnitude of the change in the MMA of the DHA:DSPC monolayers was significantly less than that measured for VLC-PUFA at 9 and 6 $Å^2$/lipid for 0.1 and 1 mol % DHA, respectively, Fig. 3. These results suggest that the polyunsaturated portion of VLC-PUFA must be *embedded* in the DSPC monolayer, as opposed to the polyunsaturated portion extending *beyond* the monolayer, to account for the large increase in the MMA observed at low fractions of VLC-PUFA in DSPC. It has been postulated that DHA can fold and form hairpin-like structures in lipid membranes (38) which by analogy, the polyunsaturated

Please cite this article in press as: Cheng et al., Influence of very-long-chain polyunsaturated fatty acids on membrane structure and dynamics, Biophysical Journal (2022), https://doi.org/10.1016/j.bpj.2022.06.015

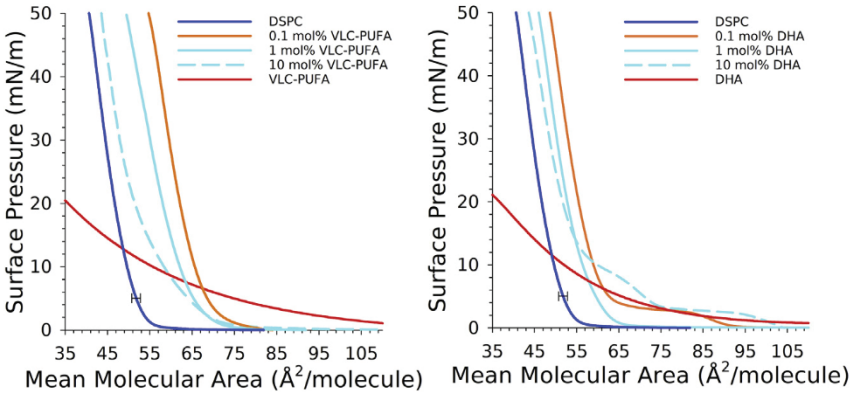

FIGURE 2 (Left) π-A isotherms of at 0 mol % (*dark blue*), 0.1% (*orange*), 1% (*cyan*), 10% (*dashed line*, *cyan*), and 100% VLC-PUFA (*red*) in a DSPC monolayer. (Right) π-A isotherms of DHA at 0 mol % (*dark blue*), 0.1% (*orange*), 1% (*cyan*), 10% (*dashed line*, *cyan*), and pure DHA (*red*) in a DSPC monolayer. The error bar on the DSPC isotherm is representative of the standard deviation from triplicate measurements. All isotherms were collected over a PBS pH 7.4 subphase at 22°C. The isotherms show are the average of at least three independent compression experiments. To see this figure in color, go online.

portion of VLC-PUFAs must re-insert into the membrane giving rise to the larger measured MMAs. In comparison, a linear chain conformation would allow for the PUFA tail to extend into the opposing leaflet in a lipid bilayer (39–41), so the trends observed here may not fully describe the behavior in a lipid bilayer.

Both the VLC-PUFA + DSPC and DHA + DSPC binary mixtures exhibit an increase in the MMA of the lipids in the membrane. Mixtures of 1-palmitoyl-2-docosahexaenoyl-*sn*-glycero-3-phosphocholine (PDPC) and DPPC also exhibit an increasing in the lipid MMA over DPPC alone (42). From the reported isotherms, the MMA of a 1:5 PDPC:DPPC mixture (10 mol % DHA) was roughly 57 Å^2/molecule at 20 mN/m, which is similar to the measured MMA of 52.5 ± 0.4 Å^2/molecule of the 10 mol % VLC-PUFA:DSPC monolayer (Fig. 2). The agreement between the MMAs of 10 mol % VLC-PUFA:DSPC and 20 mol % PDPC:DPPC also support the hypothesis that the DHA portion contributes significantly to the MMA of VLC-PUFA, implying that DHA chain is intercalated in the DSPC monolayer in a hairpin structure. However, the contribution to the saturated myristyl chain of VLC-PUFA must contribute to the increased MMA of VLC-PUFA + DSPC membranes as the area increase is significantly greater, 6 and 5 Å^2/lipid at 0.1 and 1 mol % VLC-PUFA, respectively, compared with DHA alone.

The miscibility and energetics of mixing between VLC-PUFA and DSPC in the presence of 0.1, 1, and 10 mol % VLC-PUFA were determined by comparing the measured MMAs to the MMAs of an ideal mixture, which is the weighted average of the two components (43).

$$A_{12} = A_1X_1 + A_2X_2, \quad (13)$$

where A_{12} is the theoretical MMA, A_1 and A_2 are the mean molecular areas of components 1 and 2, respectively, and X_1 and X_2 are the mol fractions of each component. The observed positive deviations from ideal behavior of the VLC-PUFA:DSPC monolayers suggest that repulsive forces exist between VLC-PUFA and DSPC. The general shapes of the π-A isotherms of the VLC-PUFA:DSPC mixtures point to miscibility between VLC-PUFA and DSPC with no apparent phase segregation in the range of 10–50 mN/m) as evidenced by the lack of a plateaus in the isotherms and their continuous nature.

To determine whether the observed increases in MMA of VLC-PUFA:DSPC mixtures is attributable to the presence of DHA in the membrane, the MMAs of DHA:DSPC

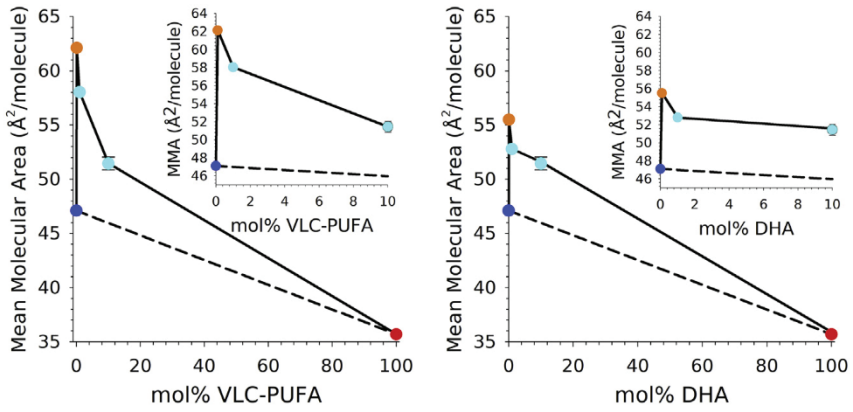

FIGURE 3 (Left) The MMAs of VLC-PUFA:DSPC and (right) DHA:DSPC monolayers at 20 mN/m, obtained from the π-A isotherms in Figure 1, for DPSC (*blue*), 0.1 mol % (*orange*), 1 mol %, and 10 mol % (*cyan*) and 100% VLC-PUFA or DHA from Eq. 13. The dashed line represents the ideal MMAs of VLC-PUFA:DSPC and DHA:DSPC mixtures. (Insets) An enhanced view of the MMAs of 0.1, 1, and 10 mol % VLC-PUFA:DSPC and DHA:DSPC monolayers. Representative errors are shown for 10 mol %. The errors were determined from triplicate isotherms. To see this figure in color, go online.

Please cite this article in press as: Cheng et al., Influence of very-long-chain polyunsaturated fatty acids on membrane structure and dynamics, Biophysical Journal (2022), https://doi.org/10.1016/j.bpj.2022.06.015

mixtures (at the same mol % as VLC-PUFA) were analyzed, and are shown in Fig. 3. A comparison between the MMAs of the DHA:DSPC mixtures and the VLC-PUFA:DSPC mixtures revealed that the MMAs of DHA:DSPC mixtures at 20 mN/m also shifted to a higher MMA, as illustrated in Fig. 3. More importantly, the MMAs of the DHA:DSPC mixtures positively deviated from the ideal MMA of the mixture, indicating that repulsive forces were present between DHA and DSPC in the monolayers. Beginning with DHA, the MMAs of the 0.1, 1, 10 mol % DHA in DSPC mixtures at 20 mN/m were determined to be 55.5 ± 0.6 Å^2/molecule, 52.7 ± 0.3 Å^2/molecule, and 51.6 ± 0.2 Å^2/molecule, respectively. In the corresponding VLC-PUFA:DSPC mixtures, the MMAs of the 0.1, 1, and 10 mol % VLC-PUFA in DSPC mixtures were determined to be 62.1 ± 0.3, 57.6 ± 0.2, and 51.5 ± 0.2 Å^2/molecule, respectively. Lor and Hirst proposed that the presence of DHA in DPPC membranes may induce significant structural changes in the DPPC gel phase matrix (22). The presence of DHA in DPPC membranes decreased the bilayer thickness via x-ray diffraction measurements of membranes comprising DPPC and 0.1 to 5 mol % DHA-PE (1-palmitoyl-2-docosahexaenoyl-*sn*-glycero-3-phosphoethanolamine). They proposed that the observed decrease in membrane thickness indicates that DHA remains embedded in the bilayer. When DHA does not extend into the opposing leaflet, it is possible that DHA fills space in a frustoconical shape, which would induce adjacent gel-phase DPPC molecules to tilt to accommodate the steric interactions between DHA and the palmitoyl chains. In other words, it is likely that the DHA portion of VLC-PUFA through its high degree of conformational freedom induces conformational changes in the adjacent stearyl chains of DSPC, resulting in a higher MMA of the monolayer.

It has been suggested that saturated lipids in the presence of DHA may result in transient raft domain formation due to preferential interactions between DHA molecules (44–49). At 0.1 mol % VLC-PUFA, VLC-PUFA is diluted in the DSPC matrix, where the PUFA tail must interact with the surrounding saturated stearoyl chains, and the unfavorable interaction between the two could give rise to the deviation from ideal mixing behavior observed here. However, as the mol % of VLC-PUFA increases, adjacent VLC-PUFAs can interact with each other, thereby mitigating unfavorable interactions between the polyunsaturated portion of VLC-PUFA and the saturated acyl chains of DSPC, thereby decreasing the deviation from ideal mixing behavior, as observed in Fig. 3.

Compression modulus

The impact of VLC-PUFA on the compression modulus of DSPC monolayers was also evaluated to investigate the interactions present in the mixed monolayers. The compression moduli of pure DSPC, pure VLC-PUFA, and 0.1, 1, and 10 mol % VLC-PUFA in DSPC monolayers were calculated from the π-A isotherms using the numerical derivative of the π-A isotherms using the following expression (50):

$$K(\Pi_i) = -A_i(\Pi_{i+1} - \Pi_{i-1})/(A_{i+1} - A_{i-1}), \quad (14)$$

where $i+1$ and $i-1$ indicate the interval of the running numerical derivative and are presented as a function of surface pressure in Fig. 4. A surface pressure of 30 mN/m was chosen for comparison purposes to reflect the pressure of the plasma membrane in cells and solution phase vesicles (30–35 mN/m) (51). The compression modulus at 30 mN/m of a DSPC monolayer was determined to be 280 ± 10 mN/m, which agrees well with reported values of 270–300 mN/m (50,52,53). The compression modulus of 0.1 mol % VLC-PUFA:DSPC significantly increases the compression modulus to 356 ± 8 mN/m, indicating that the membrane becomes less compressible compared with pure DSPC. For the 1 and 10 mol % VLC-PUFA:DSPC monolayers, the compression modulus decreased to 183 ± 7 and 179 ± 10 mN/m, respectively, and indicates that the membrane became more compressible as the amount of VLC-PUFA increased.

To assess whether the observed trends in the compression moduli of the VLC-PUFA:DSPC monolayers was attributable to the presence of the polyunsaturated portion of VLC-PUFA, compression moduli of DHA:DSPC monolayers were calculated and are shown in Fig. 4. Generally, increasing the amount of DHA in the DSPC monolayer decreased the compression modulus of the monolayer, indicating that the membrane becomes more compressible. The trend observed in the DHA:DSPC monolayers is consistent with the measurements and observations by Dumaual et al. (42). They studied mixtures of PDPC:DPPC monolayers, where increasing the amount of DHA in the monolayer (by increasing the amount of PDPC) decreased the compression modulus of the PDPC:DPPC monolayer. The observed decrease was attributed to a "redistribution of lipids (changes in packing) within the monolayer." Concomitant with π-A measurements, fluorescence microscopy images revealed that DPPC segregated from PDPC and formed small DPPC-rich domains at concentrations greater than 10 mol %, but did not observer noticeable phase segregation at or below this concentration, which is consistent with our observations for VLC-PUFA. In this study we did not examine concentrations greater than 10 mol % as they were not relevant to our ongoing clinical studies in mice models. Because of the repulsive forces between VLC-PUFA and DSPC, more energy would be required to force VLC-PUFA and DSPC together (i.e., higher compression modulus). At a low mol % of VLC-PUFA, the PUFA tail would necessarily interact with the stearoyl chains of DSPC. Compression of this system would require either exclusion of the PUFA tail from the monolayer, or conformational alignment of the unsaturated tail into and all-*trans*

Please cite this article in press as: Cheng et al., Influence of very-long-chain polyunsaturated fatty acids on membrane structure and dynamics, Biophysical Journal (2022), https://doi.org/10.1016/j.bpj.2022.06.015

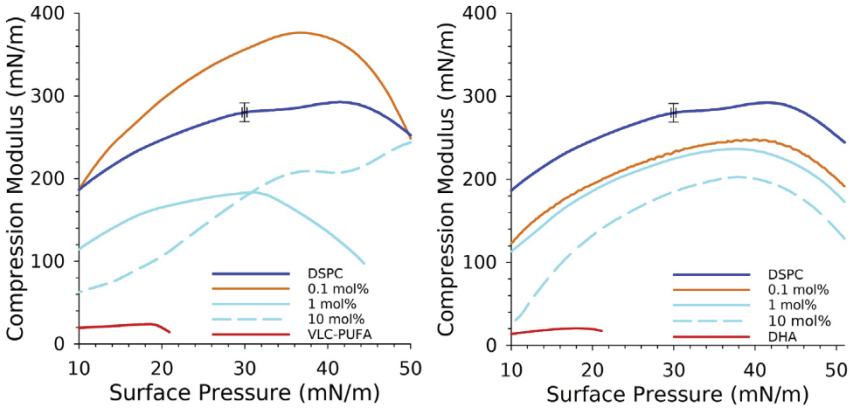

FIGURE 4 (*Left*) Compression moduli of VLC-PUFA:DSPC monolayers for the following concentrations of VLC-PUFA: 0 mol % VLC-PUFA (*blue*), 0.1 mol % (*orange*), 1 mol % (*cyan*), 10 mol % (*dashed cyan*), and 100 mol % (*red*). (*Right*) Compression moduli of DHA:DSPC monolayers for the following concentrations of DHA: 0 mol % (*blue*), 0.1 mol % (*orange*), 1 mol % (*cyan*), 10 mol % (*dashed cyan*), and 100 mol % (*red*). The error bars shown for DSPC are representative of the standard deviation obtained from triplicate measurements. To see this figure in color, go online.

configuration both of which are energetically unfavorable, and presumably responsible for the observed increase in the compressibility of the monolayer. However, at 1 and 10 mol % VLC-PUFA:DSPC, it is likely that the additional PUFA is present in the monolayer allows for more favorable interactions between the PUFA tails. Thus, the observed changes in the compression modulus and MMA support the hypothesis that the PUFA tail of VLC-PUFA inserts into the DSPC monolayer, thereby changing the compressibility of the DSPC membrane.

Excess free energy of mixing

The observed expansion of the VLC-PUFA:DSPC monolayers can be related to the excess free energy of mixing, ΔG^{exc} using the following expression (43).

$$\Delta G^{exc} = N \int_0^{\Pi_C} (A_{12} - A_1X_1 - A_2X_2)d\Pi, \qquad (15)$$

where N is Avogadro's number, and Π_C is the monolayer collapse pressure (43). Using the π-A isotherms, ΔG^{exc} was calculated by using the limits of integration from 0 to 49 mN/m, which is slightly below the collapse pressure of DSPC. The calculated ΔG^{exc} are plotted as a function of mol % VLC-PUFA in Fig. 5, and the overall positive ΔG^{exc} values for the VLC-PUFA:DSPC monolayers indicate unfavorable, repulsive forces between VLC-PUFA and DSPC. The largest ΔG^{exc} was observed for 0.1 mol % VLC-PUFA in DSPC monolayers, which is consistent with the positive deviation from ideal mixing behavior shown in Fig. 3.

To test whether the increase in ΔG^{exc} observed for VLC-PUFA can be attributed to the polyunsaturated portion of VLC-PUFA, ΔG^{exc} values for DHA:DSPC monolayers were also calculated (Fig. 5). The presence of DHA increased the free energy of mixing significantly in DHA:DSPC monolayers. The observed changes in the VLC-PUFA:DSPC mixed monolayers may be due to the presence of the "folded" PUFA chain of VLC-PUFA in the monolayer because of the structural similarity between DHA and VLC-PUFA. However, the free energies of mixing of the VLC-PUFA:DSPC mixtures were generally greater than the free energies of mixing of the DHA:DSPC mixtures. This discrepancy suggests that the presence of DHA accounts for *some* but not all of the changes observed. The myristyl chain of VLC-PUFA may play a role in the observed increase in the free energy of mixing for VLC-PUFA:DSPC monolayers.

Increasing the mol % DHA in DHA:DSPC and VLC-PUFA:DSPC monolayers decreased the magnitude of ΔG^{exc}. A lower ΔG^{exc} indicates fewer repulsive forces between VLC-PUFA and DSPC. For instance, the presence of 10 mol % VLC-PUFA:DSPC mixture had an overall smaller ΔG^{exc} (i.e., fewer repulsive interactions) than the 0.1 mol % VLC-PUFA:DSPC mixture, presumable due to the more favorable interaction of the PUFA tails with each other compared with the saturated DSPC lipid component.

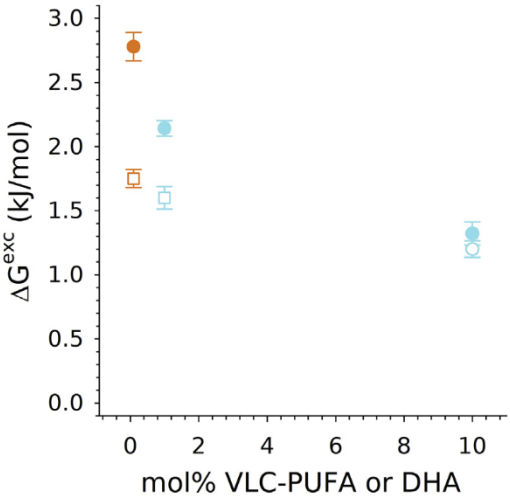

FIGURE 5 Excess free energy of mixing of mixed membranes containing VLC-PUFA (*circles*) or DHA (*squares*) in DSPC for 0.1, 1, 10 mol %. Error bars were computed by propagating the errors in the measured MMA determined from the Langmuir isotherms. To see this figure in color, go online.

Please cite this article in press as: Cheng et al., Influence of very-long-chain polyunsaturated fatty acids on membrane structure and dynamics, Biophysical Journal (2022), https://doi.org/10.1016/j.bpj.2022.06.015

Lipid chain ordering

In addition to changes in mechanical properties of DSPC monolayers in the presence of VLC-PUFA, the impact of VLC-PUFA on DSPC acyl chain ordering was also studied using SFVS. SFVS spectra of the acyl chain region of the DSPC component in PSLBs provided molecular-level details on the impact of VLC-PUFA on acyl chain structure (Fig. 6). The studies hereafter focus only on the 0.1 mol % VLC-PUFA:DSPC mixture, as VLC-PUFA is at similar concentrations in the retina (17) and the most pronounced physical changes in the monolayers were observed for this concentration. The observed peaks in the spectra shown in Fig. 6, agree well with previously established SFVS spectra of the acyl chain region of DSPC: CH_2 ν_S (2847 cm^{-1}), CH_3 ν_S (2875 cm^{-1}), CH_2 ν_{AS} (2898 cm^{-1}), CH_3 ν_{FR} (2936 cm^{-1}), and CH_3 ν_{AS} (2960 cm^{-1}) (30).

By taking the ratio of the integrated areas of the CH_2 ν_S and CH_3 ν_S peaks, the SFVS spectra can shed light on the effect of VLC-PUFA on acyl chain order. When using the *ssp* polarization combination, the CH_2 ν_S for an all-*trans* configuration of the acyl chains is forbidden, but as the chains become more disordered, the CH_2 ν_S gains intensity through a break in the local symmetry of the acyl chain backbone (54–57). A relative measure of acyl chain disorder is obtained from the ratio of the CH_2 ν_S/CH_3 ν_S modes. The calculated CH_2 ν_S/CH_3 ν_S ratios for an asymmetric DSPC bilayer in the absence of 0.1 mol % VLC-PUFA were determined to be 0.27 ± 0.07. In the presence of 0.1 mol % VLC-PUFA in both leaflets, the calculated CH_2 ν_S/CH_3 ν_S ratio was determined to be 0.5 ± 0.1.

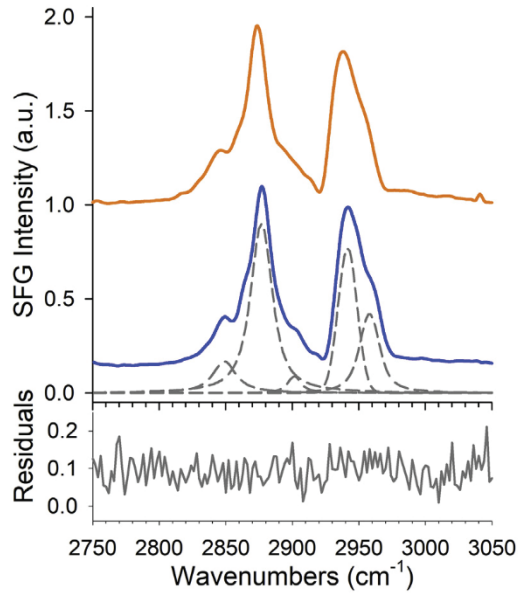

FIGURE 6 (*A*) SFVS spectra of pure DSPC (*blue*), DPSC +0.1 mol % VLC-PUFA (*orange*) obtained using the *ssp* polarization combination in PBS in D_2O at room temperature. The spectra were normalized to the CH_3 ν_S peak and offset for clarity. The fits to the vibrational modes corresponding to the acyl chains are shown (*dashed gray*), with the residuals from the fit shown below the spectra. To see this figure in color, go online.

The calculated CH_2/CH_3 ν_s ratio for an asymmetric DSPC PSLB is in good agreement with previous SFVS measurements that reported values around 0.3 ± 0.1 (30). In the presence of VLC-PUFA in both leaflets, the CH_2 ν_S/CH_3 ν_S ratio increases by ~0.2, indicating that the amount of *gauche* content in the acyl chains increases (i.e., higher chain disorder) in both PSLB compositions. The increase in chain disorder is consistent with the π-A isotherms, which showed a larger MMA for 0.1 mol % VLC-PUFA. The increased MMA allows for more conformational freedom within the acyl chains of DSPC, resulting in more *gauche* conformers. The increased chain disorder observed here upon the addition of VLC-PUFA is also in good agreement with ^2H NMR studies of DHA:DPPC multilamellar membranes that demonstrated a decrease in phospholipid acyl chain ordering (39,40).

It has been proposed that VLC-PUFA plays a significant role in the structure of retinal membranes, but its precise orientation within the membrane has been elusive. PSLBs containing only $DSPCd_{70}$ in the proximal leaflet and 0.1, 1, and 10 mol % and 50 mol % VLC-PUFA in $DSPCd_{70}$ in the proximal leaflet were made. Despite the high concentration of VLC-PUFA in the PSLB, no measurable SFVS was found. Because the SFVS response is proportional to the average molecular orientations (Eq. 4), highly disordered or randomly oriented molecules will result in a very low SFVS signal. Thus, the SFVS spectrum of VLC-PUFA (or lack thereof) would suggest that VLC-PUFA is oriented randomly in the membrane.

Since no measurable signal of VLC-PUFA could be obtained, the effect of VLC-PUFA on DSPC, which has a measurable vibrational signature (CH_3 ν_S), was examined. Specifically, VLC-PUFA affected the structure of the surrounding DSPC matrix—such as chain disorder and potentially inducing tilts of gel-phase DSPC molecules—and free energy of mixing in VLC-PUFA:DSPC membranes by way of DHA. Whether VLC-PUFA affected DSPC flip-flop kinetics was measured and examined next.

DSPC flip-flop

The presence of VLC-PUFA suggested that the PUFA tail shapes the physical properties of VLC-PUFA:DSPC PSLBs, and how these differences are manifested in the dynamics of flip-flop was investigated using SFVS. The DSPC flip-flop rates were calculated from the CH_3 ν_S intensity profiles over time by fitting Eq. 12 to the data and are presented in Table 1 and Fig. 7. The half-lives of flip-flop were calculated using the expression:

$$t_{1/2} = \frac{\ln(2)}{2k} \tag{16}$$

where k is the rate determined Eq. 12. The calculated $t_{1/2}$ for DSPC flip-flop are listed in Table 1.

Please cite this article in press as: Cheng et al., Influence of very-long-chain polyunsaturated fatty acids on membrane structure and dynamics, Biophysical Journal (2022), https://doi.org/10.1016/j.bpj.2022.06.015

A comparison of the flip-flop rates of pure DSPC and 0.1 mol % VLC-PUFA at 46°C is presented in Fig. 8. At this temperature, the half-life of DSPC flip-flop in the absence of VLC-PUFA was 120 ± 2 min in PBS in D_2O, which is in good agreement with the previously determined half-life of 124 ± 1 min (52). The incorporation of 0.1 mol % VLC-PUFA significantly increased the DSPC flip-flop rate (i.e., faster) with a calculated half-life of 24.3 ± 0.2 min at 45.8 ± 0.3°C. This reduction in the half-life of DSPC flip-flop is consistent with a previous study of lipid flip-flop in vesicles containing NBD-PE (1,2-dipalmitoyl-sn-glycero-3-phosphoethanolamine-N-(7-nitro-2-1,2-benzo xadazol-4-yl)) and DHA by Armstrong et al. (58). The measured half-life of NBD-PE without DHA was approximately 11.5 h, but in the presence of 20 mol % DHA, the half-life was dramatically reduced to 0.23 h (14 min). While there are differences in the magnitudes of the rates, the observed relative reduction in the rate in the presence of DHA agrees well with the rates presented here and strongly suggests that the PUFA tail of VLC-PUFA accelerates DSPC flip-flop in the VLC-PUFA:DSPC membranes compared with pure DSPC membranes. The authors note that the studies presented herein are the first biophysical measurements of model membranes comprising synthetic VLC-PUFAs in a phospholipid matrix, as sufficient quantities of pure VLC-PUFAs could not obtained until now.

The apparent increase in the rate of DSPC flip-flop in the presence of VLC-PUFA could be a consequence of the changes in membrane packing, and we have previously demonstrated that phospholipids with higher MMAs flip-flop faster (59,60). In brief, the flip-flop rate depends on surface packing. Because the surface pressure and MMAs are related through the π-A isotherms, the flip-flop rate can also be described as a function of MMA at a fixed temperature. In the 0.1 mol % VLC-PUFA:DSPC mixture, the MMA of the membrane is 61.3 ± 0.1 $Å^2$/molecule (Fig. 2) at 30 mN/m. Using the previously determined relationship between the surface pressure and rate of DSPC flip-flop (60) the theoretical half-life of DSPC flip-flop would be 45 ± 5 min after accounting for differences in the MMA of DSPC. Using the rates from Table 1, the extrapolated half-life of DSPC flip-flop was determined to be 110 ± 10 min at 40°C, which is roughly 2.4 times slower than the theoretical half-life of DSPC flip-flop. It is also possible that the alteration of the rate of DSPC flip-flop is due in part to membrane defects introduced by VLC-PUFA components, which is supported by the measured chain disorder in DSPC. In either case, these results suggest that a small mol % of VLC-PUFA can result in dramatic changes in lipid flip-flop rates. The fact that VLC-PUFA improves lipid translocation, makes it noteworthy in retinal membranes where there is high influx of retinoids. This enhancement of flip-flop by VLC-PUFAs provides an alternative non-enzymatic mechanism for retinoid translocation in

TABLE 1 The measured rates and half-lives of the DSPC CH_3 ν_S decay over time at various temperatures

Temperature (°C)	Rate (k) × 10^5 (s^{-1})	$t_{1/2}$ (min)
36.6 ± 0.2	1.93 ± 0.01	299 ± 1
41.55 ± 0.07	7.82 ± 0.05	73.9 ± 0.5
44.0 ± 0.1	18.46 ± 0.01	31.29 ± 0.02
45.8 ± 0.3	23.8 ± 0.2	24.3 ± 0.2
48.1 ± 0.2	127 ± 5	4.6 ± 0.2

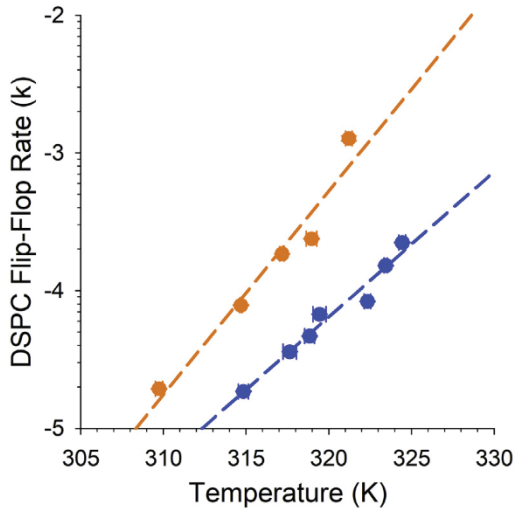

FIGURE 7 Comparison of the measured DSPC flip-flop rates as a function of temperature of pure DSPC (*blue*) and 0.1 mol % VLC-PUFA (*orange*). The data for pure DSPC flip-flop were taken from (35). Vertical error bars represent the error obtained from the nonlinear regression used to determine the rate of flip-flop while the horizontal error is due to the uncertainty in the measured temperature at which the flip-flop decay data was obtained. To see this figure in color, go online.

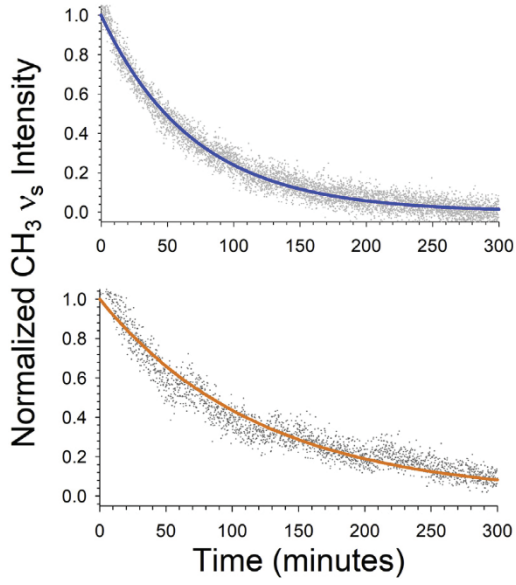

FIGURE 8 Intensity of the CH_3 ν_S of DSPC as a function of time of an asymmetric DSPC bilayer (top, *blue*) and 0.1 mol % VLC-PUFA:DSPC (bottom, *orange*) at 46°C in PBS in D_2O. To see this figure in color, go online.

photoreceptors, in addition to translocation mediated by the ABCA4 enzyme (28).

CONCLUSIONS AND FUTURE DIRECTIONS

The influence of VLC-PUFA (C32:6 n-3) on the biophysical properties of a model DSPC membrane were investigated, specifically membrane packing, compressibility, lipid chain ordering, and lipid flip-flop rates. To what extent the observed changes in membrane properties upon the addition of VLC-PUFA could be attributed to the pendent polyunsaturated chain of VLC-PUFA, the same measurements were conducted on DHA:DSPC mixed monolayers. The influence of VLC-PUFA on membrane packing was analyzed from π-A isotherms of 0.1, 1, and 10 mol % VLC-PUFA in DSPC and compared with the corresponding DHA:DSPC mixed monolayers because of the structural similarity between DHA and the PUFA portion of VLC-PUFA. The MMA of DSPC:VLC-PUFA monolayers greatly expanded in the presence of VLC-PUFA, demonstrating that VLC-PUFA:DSPC mixed membranes deviate from ideal mixing behavior. DHA:DSPC mixed membranes also deviated from ideal mixing behavior, suggesting that the changes in membrane structure could be attributable in large part to the PUFA portion of VLC-PUFA. The expansion is postulated to occur because of insertion of the PUFA tail into the monolayer and the conformational freedom imparted by the PUFA tail allowing it to adopt a hairpin structure in the lipid monolayer. The influence of VLC-PUFA on the compression modulus showed that 0.1 mol % VLC-PUFA made the VLC-PUFA:DSPC membrane harder to compress. By contrast, the change in compression modulus of the 1 and 10 mol % VLC-PUFA:DSPC membranes is consistent with the behavior observed in DHA:DSPC mixed membranes, which indicates that the pendent PUFA chain is intercalated within the monolayer and plays a significant role determining the membranes' mechanical properties. In addition to the changes in the compression moduli, the magnitude of free energy of mixing (ΔG^{exc}) was found to decrease as a function of increasing mol % VLC-PUFA, which may be attributable to phase segregation between of VLC-PUFA-rich regions in the monolayer via stabilizing interactions between PUFA tails. In addition to the LB measurements, the SFVS spectra illustrated that the DSPC acyl chains become more disordered in the presence of VLC-PUFA, supporting the observed expansion of the VLC-PUFA:DSPC membrane. The changes in the physical properties of the VLC-PUFA:DSPC monolayers were also apparent in the dynamics of DSPC flip-flop. After accounting for the differences in the MMAs of DSPC, the observed increase in DSPC flip-flop could be largely attributed to packing differences induced by VLC-PUFA. These results show the first direct measurement of the impact of VLC-PUFA on the physical properties of model membranes on the molecular level and how these may impact lipid flip-flop dynamics. 0.1 mol % of VLC-PUFA induces a dramatic change in lipid membrane structure and dynamics. Relatively low levels of VLC-PUFAs (0.1 mol %) in DSPC membranes result in high membrane rigidity, which makes the membranes less susceptible to compression. VLC-PUFA also improves lipid translocation, which makes them noteworthy in retinal membranes where there is high influx of retinoids.

The authors note that the studies presented herein correspond to *free* VLC-PUFA in model membranes. Biophysical measurements on VLC-PUFA integrated into a phospholipid in the *sn*-2 position would complement the studies presented herein as VLC-PUFAs are principally incorporated into phospholipids of the ROS (1,10). Studies are underway to synthetically produce VLC-PUFA incorporated into a phospholipid at either the *sn*-1 or *sn*-2 position, which has been postulated to bear biological significance. For instance, Aveldano proposed that incorporation of VLC-PUFAs in the *sn-1* position enabled tight binding between VLC-PUFA phospholipids and rhodopsin (where VLC-PUFA phospholipids are difficult to separate from rhodopsin) (19). When these lipids have been synthesized, further experiments on model membranes will be conducted to complement the work presented in this study.

AUTHOR CONTRIBUTIONS

J.C.C., P.S.B., and J.D.R. conceived the idea for the manuscript and secured funding support for the published work. R.R. and S.L. synthesized the VLC-PUFA (C32:6 n-3) used in this study. A.G. and G.R. assisted in identifying the composition of the VLC-PUFA used in this study and aided in the analysis in relation to in vivo studies they conducted. V.C. and J.C.C. designed the experiments described in the manuscript, performed the data analysis of experimental results, and wrote the manuscript. V.C., J.C.C., P.S.B., J.D.R., and A.G. contributed to editing the manuscript.

ACKNOWLEDGMENTS

Supported by Foundation Fighting Blindness grant no. TA-NMT-0618-0736-UUT, NIH grant EY-14800, NSF grant 1953975 and an unrestricted departmental grant from Research to Prevent Blindness.

DECLARATION OF INTERESTS

The authors declare no competing interests.

REFERENCES

1. Aveldaño, M. I. 1987. A novel group of very long chain polyenoic fatty acids in dipolyunsaturated phosphatidylcholines from verte-brate retina. *J. Biol. Chem.* 262:1172–1179. https://doi.org/10.1016/s0021-9258(19)75767–6.

2. Aveldaño, M. I., and H. Sprecher. 1987. Very long chain (C24 to C36) polyenoic fatty acids of the n-3 and n-6 series in dipolyunsatu- rated phosphatidylcholines from bovine retina. *J. Biol. Chem.* 262:1180–1186. https://doi.org/10.1016/s0021-9258(19)75768-8.

3. Bennett, L. D., R. S. Brush, …, R. E. Anderson. 2014. Effect of reduced retinal VLC-PUFA on rod and cone photoreceptors. *Invest. Ophthalmol. Vis. Sci.* 55:3150. https://doi.org/10.1167/iovs.14-13995.

4. Liu, A., J. Chang, …, P. S. Bernstein. 2010. Long-chain and very long-chain polyunsaturated fatty acids in ocular aging and age-related macular degeneration. *J. Lipid Res.* 51:3217–3229. https://doi.org/10.1194/jlr.m007518.
5. Marchette, L. D., D. M. Sherry, …, N. A. Mandal. 2014. Very long chain polyunsaturated fatty acids and rod cell structure and function. *Adv. Exp. Med. Biol.* 801:637–645. https://doi.org/10.1007/978-1-4614-3209-8_80.
6. Poulos, A., P. Sharp, …, A. Poulos. 1988. The occurrence of polyenoic very long chain fatty acids with greater than 32 carbon atoms in molecular species of phosphatidylcholine in normal and peroxisome-deficient (Zellweger's syndrome) brain. *Biochem. J.* 253:645–650. https://doi.org/10.1042/bj2530645.
7. Robinson, B. S., D. W. Johnson, …, A. Poulos. 1990. Metabolism of hexacosatetraenoic acid (C26:4, n-6) in immature rat brain. *Biochem. J.* 267:561–564. https://doi.org/10.1042/bj2670561.
8. Rezanka, T. 1989. Very-long-chain fatty acids from the animal and plant kingdoms. *Prog. Lipid Res.* 28:147–187. https://doi.org/10.1016/0163-7827(89)90011-8.
9. Tvrzická, E., T. Rezanka, …, V. Janousek. 1988. Identification of very-long-chain fatty acids in rat and mouse harderian gland lipids by capillary gas chromatography-mass spectrometry. *J. Chromatogr.* 431:231–238. https://doi.org/10.1016/s0378-4347(00)83092-3.
10. Poulos, A. 1995. Very long chain fatty acids in higher animals–a review. *Lipids.* 30:1–14. https://doi.org/10.1007/bf02537036.
11. Agbaga, M. P., S. Logan, …, R. E. Anderson. 2014. Biosynthesis of very long-chain polyunsaturated fatty acids in hepatocytes expressing ELOVL4. *Adv. Exp. Med. Biol.* 801:631–636. https://doi.org/10.1007/978-1-4614-3209-8_79.
12. Bennett, L. D., and R. E. Anderson. 2016. Current progress in deciphering importance of VLC-PUFA in the retina. *Adv. Exp. Med. Biol.* 854:145–151. https://doi.org/10.1007/978-3-319-17121-0_20.
13. Harkewicz, R., H. Du, …, K. Zhang. 2012. Essential role of ELOVL4 protein in very long chain fatty acid synthesis and retinal function. *J. Biol. Chem.* 287:11469–11480. https://doi.org/10.1074/jbc.M111.256073.
14. Bernstein, P. S., J. Tammur, …, A. Hutchinson. 2001. Diverse macular dystrophy phenotype caused by a novel complex mutation in the ELOVL4 gene. *Invest. Ophthalmol. Vis. Sci.* 42:3331–3336. http://www.ncbi.nlm.nih.gov/pubmed/11726641.
15. Zhang, K., M. Kniazeva, …, K. Petrukhin. 2001. A 5-bp deletion in ELOVL4 is associated with two related forms of autosomal dominant macular dystrophy. *Nat. Genet.* 27:89–93. https://doi.org/10.1038/83817. http://www.ncbi.nlm.nih.gov/pubmed/11138005.
16. Gorusupudi, A., A. Liu, …, P. S. Bernstein. 2016. Associations of human retinal very long-chain polyunsaturated fatty acids with dietary lipid biomarkers. *J. Lipid Res.* 57:499–508. https://doi.org/10.1194/jlr.p065540.
17. Liu, A., J. Chang, …, P. S. Bernstein. 2009. Enhanced methods for analysis of very long chain polyunsaturated fatty acids from retina and RPE. *Invest. Ophthalmol. Vis. Sci.* 50:3410.
18. Bennett, L. D., B. R. Hopiavuori, …, R. E. Anderson. 2014. Examination of VLC-PUFA-deficient photoreceptor terminals. *Invest. Ophthalmol. Vis. Sci.* 55:4063. https://doi.org/10.1167/iovs.14-13997.
19. Aveldano, M. I. 1988. Phospholipid species containing long and very long polyenoic fatty acids remain with rhodopsin after hexane extraction of photoreceptor membranes. *Biochemistry.* 27:1229–1239. https://doi.org/10.1021/bi00404a024.
20. Bruno, M. J., R. E. Koeppe, and O. S. Andersen. 2007. Docosahexaenoic acid alters bilayer elastic properties. *Proc. Natl. Acad. Sci. USA.* 104:9638–9643. https://doi.org/10.1073/pnas.0701015104.
21. Feller, S. E., K. Gawrisch, and T. B. Woolf. 2003. Rhodopsin exhibits a preference for solvation by polyunsaturated docosohexaenoic acid. *J. Am. Chem. Soc.* 125:4434–4435. https://doi.org/10.1021/ja0345874.
22. Lor, C., and L. Hirst. 2015. Effects of low concentrations of docosahexaenoic acid on the structure and phase behavior of model lipid membranes. *Membranes.* 5:857–874. https://doi.org/10.3390/membranes5040857.
23. Sander, C. L., A. E. Sears, …, K. Palczewski. 2021. Dissecting lipid contents in the distinct regions of native retinal rod disk membranes. Preprint at bioRxiv. https://doi.org/10.1101/2021.01.11.426250.
24. Hopiavuori, B. R., R. E. Anderson, and M. P. Agbaga. 2019. ELOVL4: very long-chain fatty acids serve an eclectic role in mammalian health and function. *Prog. Retin. Eye Res.* 69:137–158. https://doi.org/10.1016/j.preteyeres.2018.10.004. https://www.ncbi.nlm.nih.gov/pubmed/30982505.
25. Gorusupudi, A., R. Rallabandi, …, P. S. Bernstein. 2021. Retinal bioavailability and functional effects of a synthetic very-long-chain polyunsaturated fatty acid in mice. *Proc. Natl. Acad. Sci. USA.* 118. e2017739118. https://doi.org/10.1073/pnas.2017739118. https://www.pnas.org/content/pnas/118/6/e2017739118.full.pdf.
26. McMahon, A., and W. Kedzierski. 2010. Polyunsaturated very-long-chain C28–C36 fatty acids and retinal physiology. *Br. J. Ophthalmol.* 94:1127–1132. https://doi.org/10.1136/bjo.2008.149286.
27. Suh, M., A. A. Wierzbicki, …, M. T. Clandinin. 2000. Dietary 20:4n-6 and 22:6n-3 modulates the profile of long- and very-long-chain fatty acids, rhodopsin content, and kinetics in developing photoreceptor cells. *Pediatr. Res.* 48:524–530. https://doi.org/10.1203/00006450-200010000-00017.
28. Quazi, F., and R. S. Molday. 2013. Differential phospholipid substrates and directional transport by ATP-binding cassette proteins ABCA1, ABCA7, and ABCA4 and disease-causing mutants. *J. Biol. Chem.* 288:34414–34426. https://doi.org/10.1074/jbc.M113.508812. https://www.ncbi.nlm.nih.gov/pubmed/24097981.
29. Wade, A., R. Rallabandi, …, J. D. Rainier. 2021. The synthesis of the very long chain polyunsaturated fatty acid (VLC-PUFA) 32:6 n-3. *Org. Biomol. Chem.* 19:5563–5566. https://doi.org/10.1039/d1ob00491c.
30. Liu, J., and J. C. Conboy. 2005. Structure of a gel phase lipid bilayer prepared by the Langmuir-Blodgett/Langmuir-Schaefer method characterized by sum-frequency vibrational spectroscopy. *Langmuir.* 21:9091–9097. https://doi.org/10.1021/la051500e.
31. Allhusen, J. S., and J. C. Conboy. 2017. The ins and outs of lipid flip-flop. *Acc. Chem. Res.* 50:58–65. https://doi.org/10.1021/acs.accounts.6b00435.
32. Nakano, M., M. Fukuda, …, T. Handa. 2009. Flip-flop of phospholipids in vesicles: kinetic analysis with time-resolved small-angle neutron scattering. *J. Phys. Chem. B.* 113:6745–6748. https://doi.org/10.1021/jp900913w.
33. Gerelli, Y., L. Porcar, and G. Fragneto. 2012. Lipid rearrangement in DSPC/DMPC bilayers: a neutron reflectometry study. *Langmuir.* 28:15922–15928. https://doi.org/10.1021/la303662e.
34. Shen, Y. R. 1984. The Principles of Nonlinear Optics. Wiley-Interscience, New York.
35. Liu, J., and J. C. Conboy. 2005. 1, 2-Diacyl-phosphatidylcholine flip-flop measured directly by sum-frequency vibrational spectroscopy. *Biophys. J.* 89:2522–2532. https://doi.org/10.1529/biophysj.105.065672.
36. Smaby, J. M., M. M. Momsen, …, R. E. Brown. 1997. Phosphatidylcholine acyl unsaturation modulates the decrease in interfacial elasticity induced by cholesterol. *Biophys. J.* 73:1492–1505. https://doi.org/10.1016/S0006-3495(97)78181-5.
37. Urquhart, R., R. Y. Chan, …, W. H. Sawyer. 1992. omega-6 and omega-3 fatty acids: monolayer packing and effects on bilayer permeability and cholesterol exchange. *Biochem. Int.* 26:831–841.
38. Mitchell, D. C., S. L. Niu, …, B. M. Andersen. 2007. Effects of ROS disk membrane phospholipids with extremely long polyunsaturated acyl chains on visual signalling. *Invest. Ophthalmol. Vis. Sci.* 48:2928.
39. Eldho, N. V., S. E. Feller, …, K. Gawrisch. 2003. Polyunsaturated docosahexaenoic vs docosapentaenoic acid - differences in lipid matrix properties from the loss of one double bond. *J. Am. Chem. Soc.* 125:6409–6421. https://doi.org/10.1021/ja029029o.
40. Feller, S. E., K. Gawrisch, and A. D. MacKerell. 2002. Polyunsaturated fatty acids in lipid bilayers: intrinsic and environmental contributions

to their unique physical properties. *J. Am. Chem. Soc.* 124:318–326. https://doi.org/10.1021/ja0118340.

41. Gawrisch, K., N. V. Eldho, and L. L. Holte. 2003. The structure of DHA in phospholipid membranes. *Lipids.* 38:445–452. https://doi.org/10.1007/s11745-003-1082-0.
42. Dumaual, A. C., L. J. Jenski, and W. Stillwell. 2000. Liquid crystalline/gel state phase separation in docosahexaenoic acid-containing bilayers and monolayers. *Biochim. Biophys. Acta.* 1463:395–406. https://doi.org/10.1016/s0005-2736(99)00235-7.
43. George, L., and G. Gaines. 1996. Insoluble Monolayers at Liquid-Gas Interfaces. Springer, p. 386.
44. Levental, K. R., J. Lorent, …, I. Levental. 2016. Polyunsaturated lipids regulate membrane domain stability by tuning membrane order. *Biophys. J.* 110:1800–1810. https://doi.org/10.1016/j.bpj.2016.03.012.
45. Shaikh, S. R., J. J. Kinnun, …, S. R. Wassall. 2015. How polyunsaturated fatty acids modify molecular organization in membranes: insight from NMR studies of model systems. *Biochim. Biophys. Acta Biomembr.* 1848:211–219. https://doi.org/10.1016/j.bbamem.2014.04.020.
46. Thid, D., J. J. Benkoski, …, J. Gold. 2007. DHA-induced changes of supported lipid membrane morphology. *Langmuir.* 23:5878–5881. https://doi.org/10.1021/la700523x.
47. Wassall, S. R., M. Brzustowicz, …, W. Stillwell. 2004. Order from disorder, corralling cholesterol with chaotic lipids: the role of polyunsaturated lipids in membrane raft formation. *Chem. Phys. Lipids.* 132:79–88. https://doi.org/10.1016/s0009-3084(04)00140-9.
48. Wassall, S. R., and W. Stillwell. 2008. Docosahexaenoic acid domains: the ultimate non-raft membrane domain. *Chem. Phys. Lipids.* 153:57–63. https://doi.org/10.1016/j.chemphyslip.2008.02.010.
49. Williams, J. A., S. Batten, …, S. R. Wassall. 2012. Docosahexaenoic and eicosapentaenoic acids segregate differently between raft and non-raft domains. *Biophys. J.* 103:228–237. https://doi.org/10.1016/j.bpj.2012.06.016.
50. Smaby, J. M., V. S. Kulkarni, …, R. E. Brown. 1996. The interfacial elastic packing interactions of galactosylceramides, sphingomyelins, and phosphatidylcholines. *Biophys. J.* 70:868–877. https://doi.org/10.1016/s0006-3495(96)79629-7.
51. Marsh, D. 1996. Lateral pressure in membranes. *Biochim. Biophys. Acta Biomembr.* 1286:183–223. https://doi.org/10.1016/s0304-4157(96)00009-3.
52. Allhusen, J. S., D. R. Kimball, and J. C. Conboy. 2016. Structural origins of cholesterol accelerated lipid flip-flop studied by sum-frequency vibrational spectroscopy. *J. Phys. Chem. B.* 120:3157–3168. https://doi.org/10.1021/acs.jpcb.6b01254.
53. Gong, K., S.-S. Feng, …, P. H. Soew. 2002. Effects of pH on the stability and compressibility of DPPC/cholesterol monolayers at the air-water interface. *Colloids Surf. A Physicochem. Eng. Asp.* 270:113–125.
54. Conboy, J. C., M. C. Messmer, and G. L. Richmond. 1996. Investigation of surfactant conformation and order at the liquid-liquid interface by total internal reflection sum-frequency vibrational spectroscopy. *J. Phys. Chem.* 100:7617–7622. https://doi.org/10.1021/jp953616x.
55. Lee, C., and C. D. Bain. 2005. Raman spectra of planar supported lipid bilayers. *Biochim. Biophys. Acta.* 1711:59–71. https://doi.org/10.1016/j.bbamem.2005.02.006.
56. Miranda, P. B., V. Pflumio, …, Y. R. Shen. 1998. Chain−Chain interaction between surfactant monolayers and alkanes or alcohols at solid/liquid interfaces. *J. Am. Chem. Soc.* 120:12092–12099. https://doi.org/10.1021/ja9732441.
57. Ward, R. N., D. C. Duffy, …, C. D. Bain. 1994. Sum-frequency spectroscopy of surfactants adsorbed at a flat hydrophobic surface. *J. Phys. Chem.* 98:8536–8542. https://doi.org/10.1021/j100085a037.
58. Armstrong, V. T., M. R. Brzustowicz, …, W. Stillwell. 2003. Rapid flip-flop in polyunsaturated (docosahexaenoate) phospholipid membranes. *Arch. Biochem. Biophys.* 414:74–82. https://doi.org/10.1016/S0003-9861(03)00159-0.
59. Anglin, T. C., and J. C. Conboy. 2008. Lateral pressure dependence of the phospholipid transmembrane diffusion rate in planar-supported lipid bilayers. *Biophys. J.* 95:186–193. https://doi.org/10.1529/biophysj.107.118976.
60. Anglin, T. C., M. P. Cooper, …, J. C. Conboy. 2010. Free energy and entropy of activation for phospholipid flip-flop in planar supported lipid bilayers. *J. Phys. Chem. B.* 114:1903–1914. https://doi.org/10.1021/jp909134g.